Liquefaction Tests of Toyoura Sand Measuring Change of Quasi-elastic Deformation Properties

by

J. Koseki[1], S. Kawakami [2], H. Nagayama [3] , T. Sato [4], K. Hayano [4] and M. Torimitsu [5]

ABSTRACT

Undrained cyclic torsional and triaxial shear tests were performed on hollow cylindrical specimens of dense Toyoura sand, which were consolidated isotropically after preparation by air-pluviation. At several stress states, quasi-elastic deformation properties were measured by applying very small amplitude cyclic torsional and vertical loads. Some of the results could be explained by considering inherent and stress state-induced anisotropy in modeling of elastic deformation characteristics and by correcting for the effects of membrane penetration. Degradation in the values of elastic shear modulus and Young's modulus was observed during liquefaction when compared to those measured during isotropic consolidation.

INTRODUCTION

In analyzing the liquefaction process of sands, their elasto-plastic deformation characteristics is one of the essential aspects. On the other hand, they have not been fully revealed by laboratory tests, due to technical difficulties in very accurately evaluating elastic and plastic strain components separately. However, because of the recent developments in testing apparatuses, it became possible to measure quasi-elastic deformation properties at a strain level as small as 10^{-5} or less, as summarized by Tatsuoka et al. (1997).

For the present study, a torsional shear testing apparatus was newly introduced. In applying torsional shear stresses on the top of a hollow cylindrical specimen, it can control very small shear strains acculately. At the same time, it can also control very small vertical strains independently. Consequently, it was made possible to measure shear modulus and vertical Young's modulus of a single specimen in the quasi-elastic region.

By using this apparatus, a series of large amplitude undrained torsional and triaxial tests were performed on isotropically consolidated specimens of dense Toyoura sand, while applying very small amplitude cyclic torsional and vertical loads at a number of stress states to measure the quasi-elastic deformation properties directly. Properties measured during undrained shearing process up to liquefaction were compared to those measured during isotropic consolidation process. Some of these results were also compared to those predicted theoretically based on the hypo-elastic cross-anisotropic modeling as proposed by Tatsuoka et al. (1997).

[1] Junichi Koseki, Associate Professor, Institute of Industrial Science, University of Tokyo
[2] Sadahiro Kawakami, Graduate Student, ditto
[3] Hiroshi Nagayama, Undergraduate Student, Nihon University
[4] Takeshi Sato and Kimitoshi Hayano, Research Associate, IIS, Univ. of Tokyo
[5] Michie Torimitsu, Technical Staff, ditto

APPARATUS AND TESTING PROCEDURES

The torsional shear testing apparatus is schematically shown in Figs.1 and 2. A hollow cylindrical specimen with an outer diameter of 20 cm, inner diameter of 16 cm and a height of 30 cm were loaded in the torsional and vertical directions independently. The vertical loading parts are driven by a AC servo motor which is connected to the loading shaft through a series of reduction-gears, two sets of electro-magnetic clutch, one eletro-magnetic brake and a ball screw with a pre-pressurized nut. Refer to Santucci de Magistris et al. (1999) for the detailed performance of this vertical loading system employed for triaxial tests on solid cylindrical specimens. For the present apparatus, another set of a similar system was employed for the torsional loading parts (Fig. 2). This loading device is a displacement-controlled type from a mechanical point of view, while cyclic shear tests by keeping a specified stress amplitude can be also conducted by using a microcomputer which monitors the outputs from a load cell and controls the device accordingly.

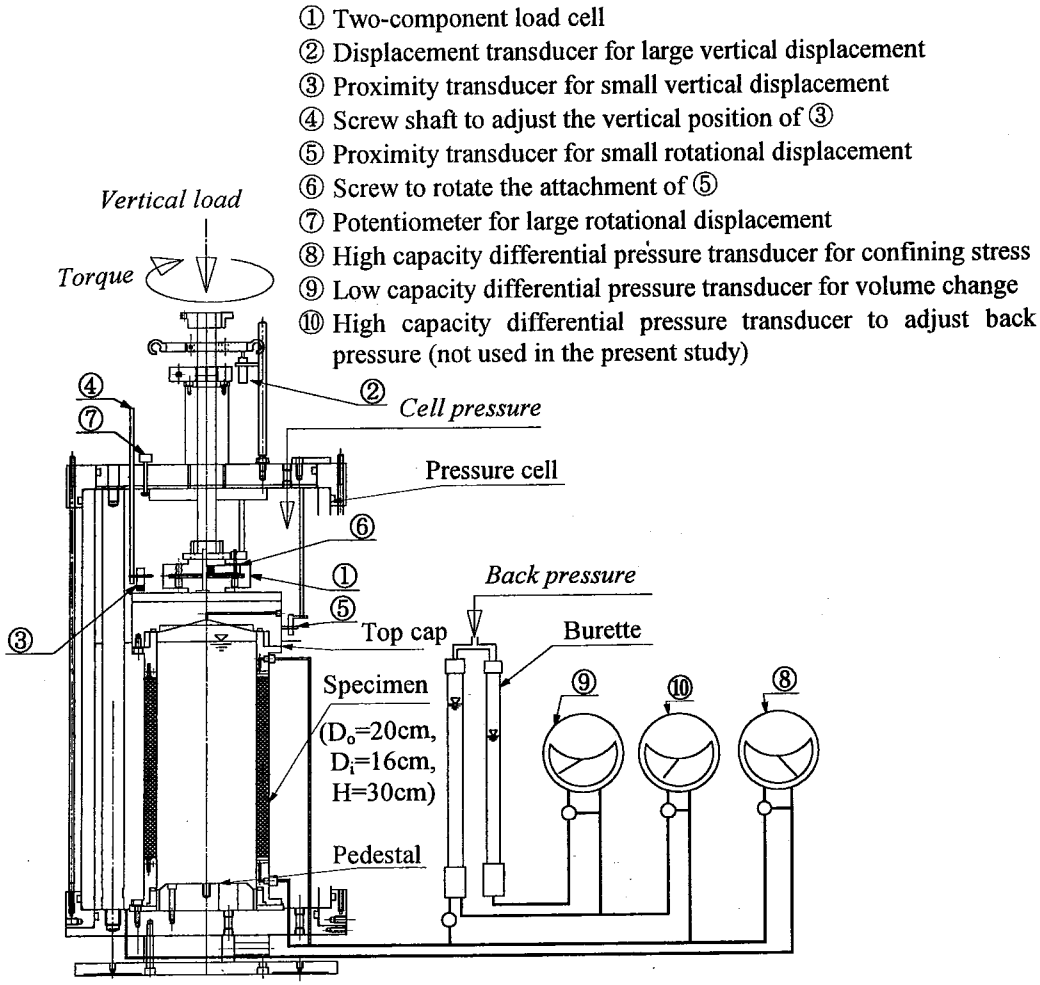

Figure 1. Torsional and triaxial testing apparatus using hollow cylindrical specimens

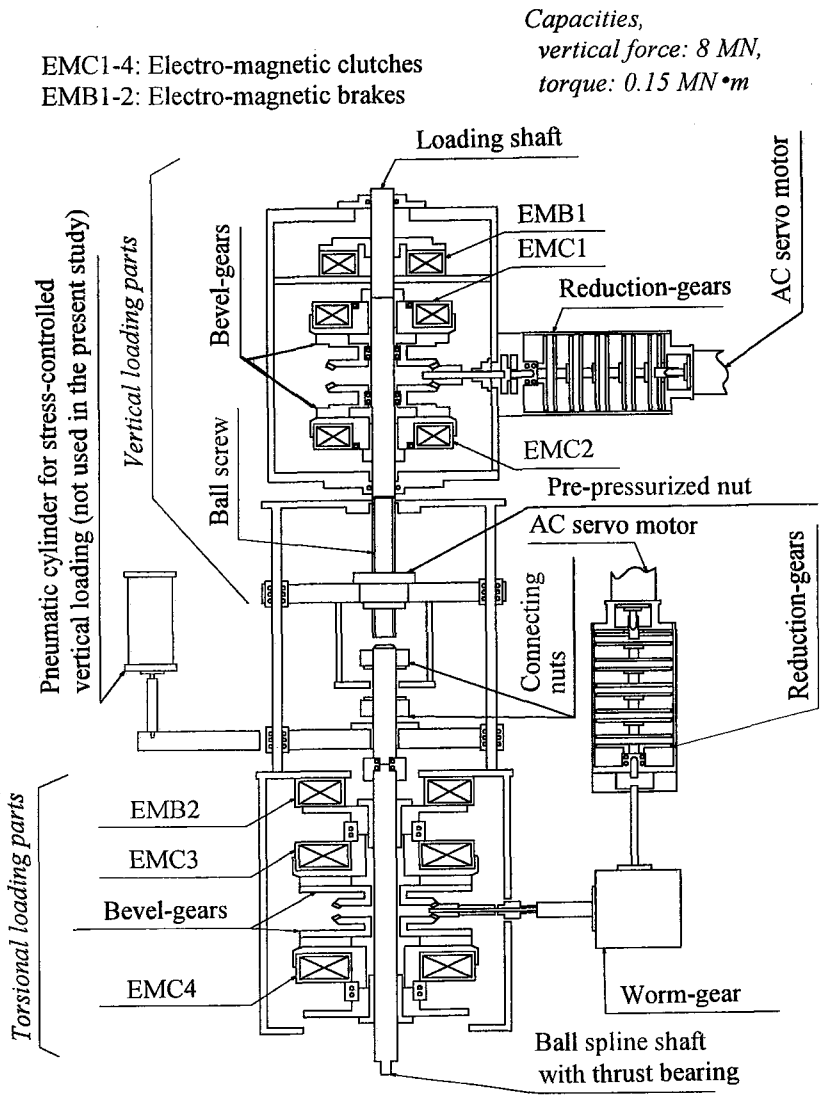

Figure 2. Torsional and vertical loading device

The tested specimens were prepared by pluviating air dried Toyoura sand (e_{max}=0.975, e_{min}=0.561) through air. They were saturated at a confining stress of 30 kPa by the double vacuuming method using partial vacuum as both the pore water pressure and the cell pressure, and were isotropically consolidated up to confining stress of $\sigma_v'=\sigma_h'$=100 kPa, where σ_v' and σ_h' denote effective vertical (or axial) and horizontal (or radial) stresses, respectively. Note that the inner and the outer cell pressures were kept equal throughout the tests so that the circumferential stress was always equal to the radial stress. The confining stress was then reduced down to about 10 kPa and restored to 100 kPa in order to investigate the behaviors at low confining stresses under isotropic stress states prior to liquefaction.

During isotropic consolidation, after some aging about 10 minutes at several stress levels, small cyclic torsional and vertical loads were applied independently, under both drained and undrained conditions with a single amplitude of about 0.0015 % and 0.0010 % for the shear strain and the vertical strain, respectively. Typical results measured under drained condition are shown in Figs. 3 and 4. The drained shear modulus G and the drained vertical Young's modulus E_v were evaluated as shown in the figures. The undrained moduli G_u and E_{vu} were evaluated in a similar manner based on the results conducted under undrained condition. It is to be noted that small cyclic isotropic loads were also applied under drained condition to evaluate the bulk modulus K, as shown in Fig. 5, which will be analyzed elsewhere.

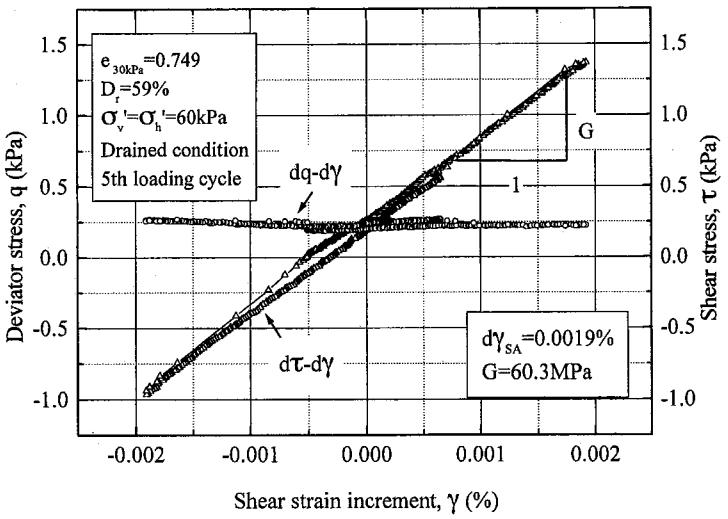

Figure 3. Typical results during drained small cyclic torsional loading at isotropic stress state

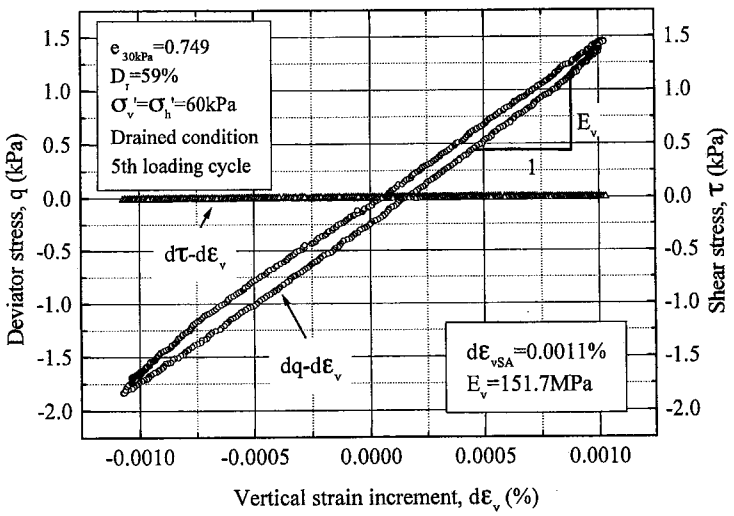

Figure 4. Typical results during drained small cyclic vertical loading at isotropic stress state

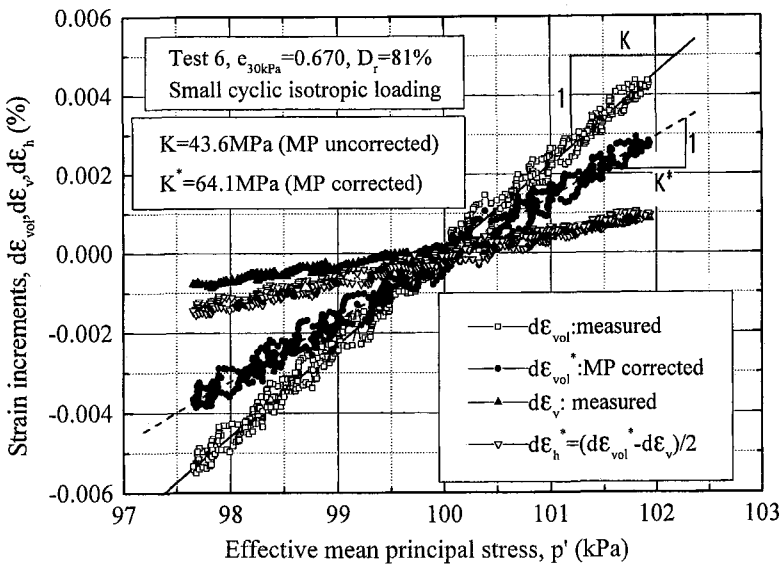

Figure 5. Typical results during drained small cyclic isotropic loading at isotropic stress state

As schematically shown in Fig. 1, the torsional and vertical loads were measured with a two-component load cell that was set inside the pressure cell to eliminate the effects of frictions between the loading shaft and the bearing of the pressure cell. The confining stress was measured with a high capacity differential pressure transducer. Proximity transducers (gap sensors) were used to evaluate small amplitude shear and vertical strains by measuring the rotational and vertical displacements of the top cap, while a potentiometer and an external displacement transducer were employed to evaluate large amplitude shear and vertical strains, respectively. A low capacity differential pressure transducer was used to evaluate volumetric strains by measuring the change of water head in a drainage burette connected to the specimen.

From isotoropic stress state with $\sigma_v' = \sigma_h' = 100$ kPa and a back pressure of 200 kPa, for one specimen denoted as test 7, the torsional load was cyclically changed under undrained condition with a single amplitude of 40 kPa for the shear stress τ, while keeping the vertical stress corrected for the change in the cross-sectional area of the specimen constant. For another specimen denoted as test 6, the vertical load was cyclically changed under undrained condition with a single amplitude of 80 kPa for the deviator stress $q = \sigma_v' - \sigma_h'$, while keeping the torsinal load to be zero. On both specimens, when the specified stress states were attained, very small amplitude unload and reload cycles were applied in the torsional and vertical directions independently, by keeping the undrained condition and without aging, with strain amplitudes that were similar to those as employed during isotropic consolidation. The stress-strain relationship and the effective stress path in these tests are shown in Figs. 6 and 7, where typical results from small cyclic loading are also shown. The undrained shear modulus G_u and the undrained vertical Young's modulus E_{vu} during shearing were evaluated as shown in these figures. It is to be noted that torsional loads were monotonically increased under drained condition in test 5 that was conducted prior to tests 6 and 7, which will be reported elsewhere, except for the vertical Young's modulus measured during isotropic consolidation as will be shown in Fig. 8 later.

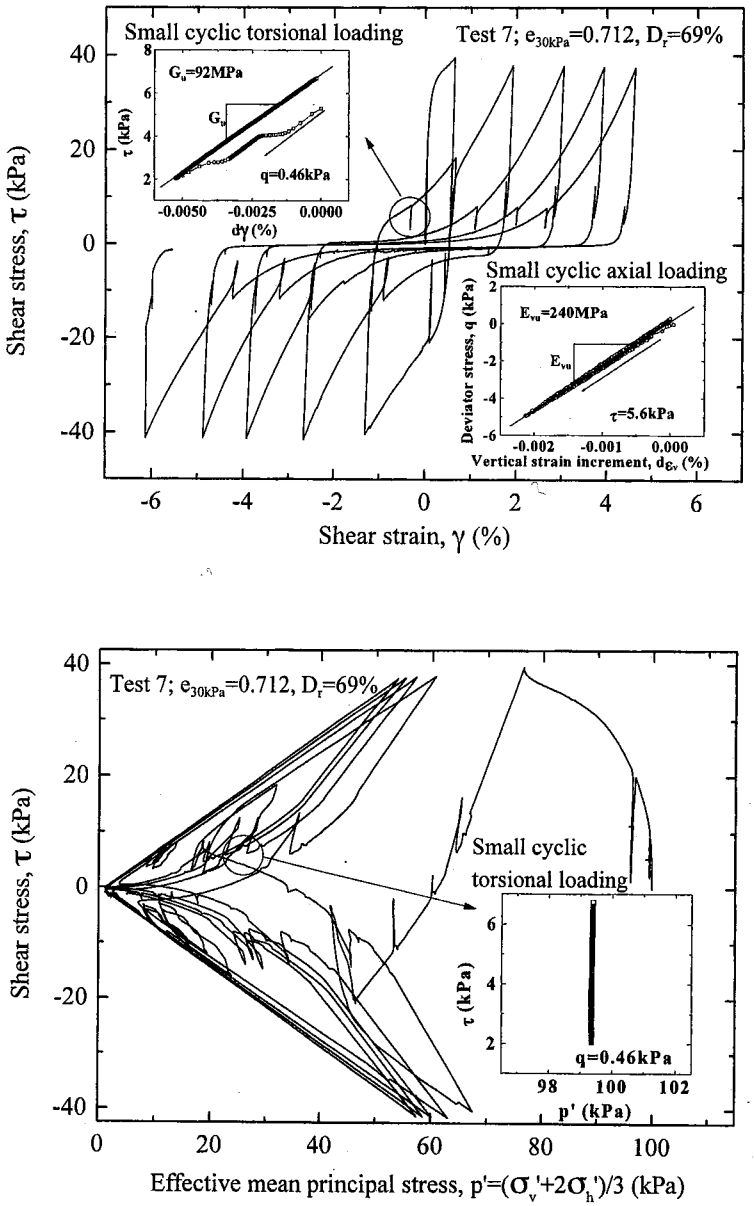

Figure 6. Results of test 7 during large amplitude undrained cyclic torsional shearing; a) stress-strain relationship; and b) effective stress path

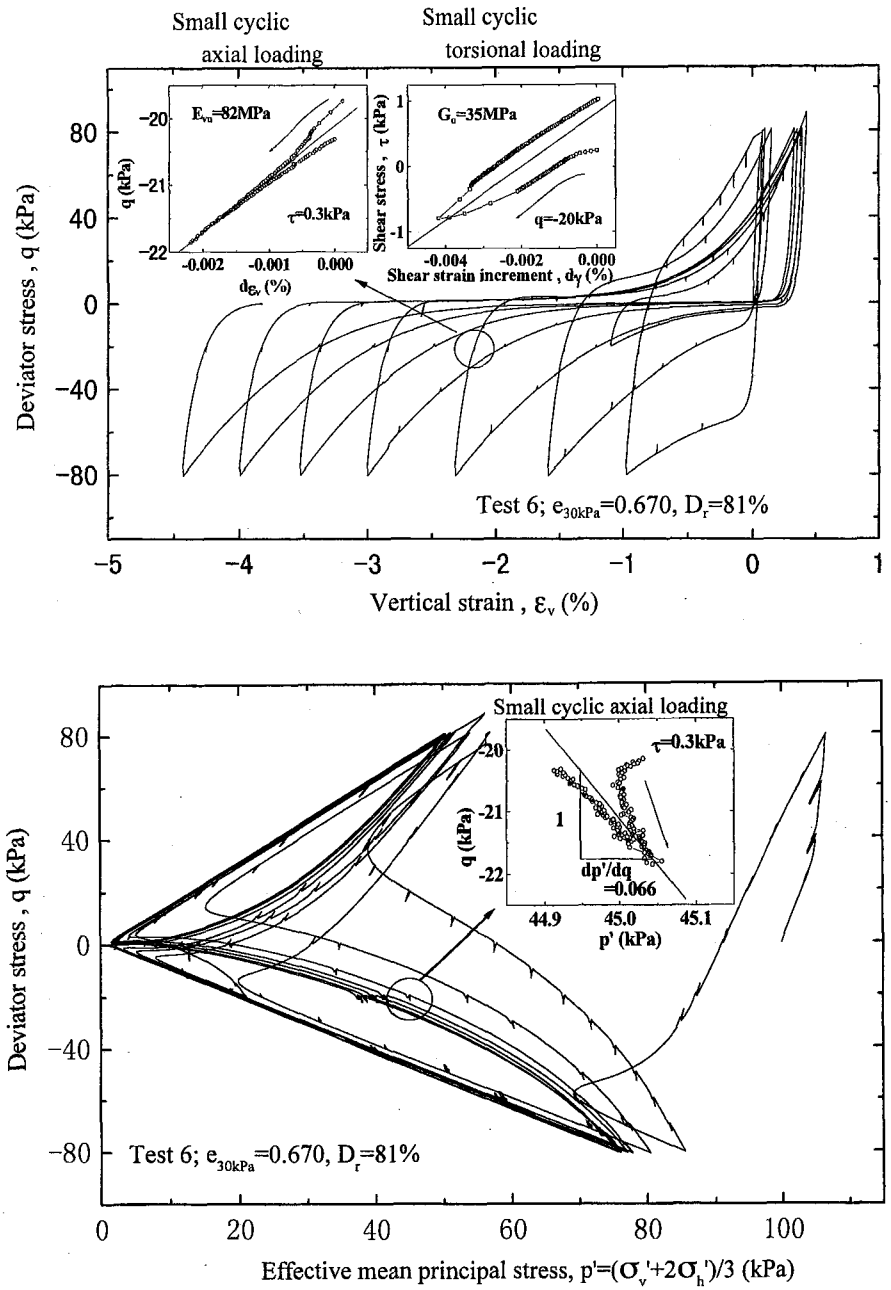

Figure 7. Results of test 6 during large amplitude undrained cyclic triaxial shearing; a) stress-strain relationship; and b) effective stress path

RESULTS AND DISCUSSIONS

Behavior during isotropic consolidation

Drained vertical Young's modulus E_v measured during isotropic consolidation was corrected for the change in the void ratio e, by dividing it with the void ratio function $f(e)=(2.17-e)^2/(1+e)$ as proposed by Hardin and Richart (1963). Relationships between the values of $E_v/f(e)$ and the confining stress were compared in Fig. 8. By making above correction, results from tests 5 through 7 conducted at different values of e in the range between 0.67 and 0.75 became almost identical. They were also similar to the results from triaxial tests using solid cylindrical specimen with a diameter of 10 cm and a height of 20 cm as reported by Koseki et al. (1998). The latter similarity demonstrates that the vertical Young's modulus can be evaluated by conducting small vertical loading on hollow cylindrical specimens in the same way as on solid cylindrical ones.

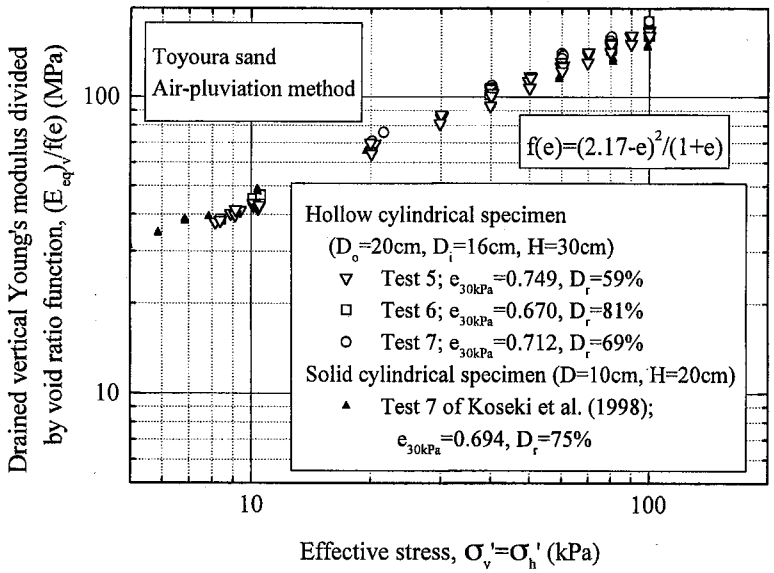

Figure 8. Drained Young's modulus versus confining stress at isotropic stress state

Measured ratios of the undrained vertical Young's modulus to the drained one, E_{vu}/E_v, are plotted versus the confining stress in Fig. 9. Theoretical relationships obtained by assuming a cross-anisotropic elastic body are also shown in the figure. Refer to Appendix for the details of the theory. It is seen that the observed behavior can be reasonably simulated by the theory with the correction for the effects of membrane penetration (hereafter denoted as MP).

The drained and undrained shear moduli, G and G_u, measured in test 6 are plotted versus the confining stress in Fig. 10. These values were almost the same irrespective of the drainage condition. In the figure, values of G_{45} and G_{45u}, based on the relationships between the shear stress and the shear strain mobilized on a plane inclined by 45 degrees from the horizontal plane, which were converted from E_v and E_{vu} by assuming the values of the drained and undrained poisson's ratios, ν and ν_u, respectively, are also shown. It is seen that the values of G_{45} were generally similar to those of G and G_u. This similarity may suggest that the effects of inherent anisotropy on shear moduli are relatively small and possibly comparable to those on the Young's

modulus for the air-pluviated specimen of Toyoura sand as have been reported by Hoque and Tatsuoka (1998), where the ratio of the vertical to horizontal Young's moduli was about 1.1 under isotropic stress states. On the other hand, the values of G_{45u} were generally smaller than the other values. This discrepancy may be partly caused by the effects of MP that resulted in underestimation of E_{vu} when these effects were neglected, as seen from Fig. 9. Similar trends of behavior were also obtained in tests 5 and 7.

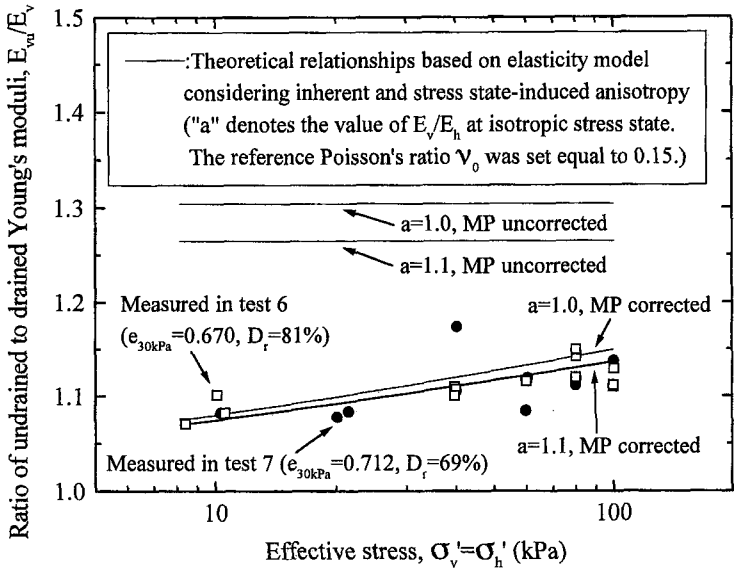

Figure 9. Ratio of undrained to drained Young's moduli at isotropic stress state

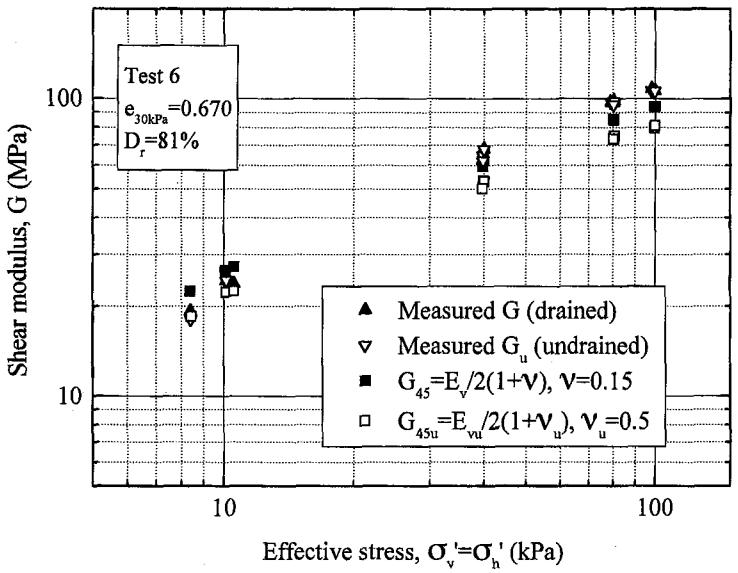

Figure 10. Drained and undrained shear moduli versus confining stress at isotropic stress state in test 6

Behavior during undrained cyclic shearing

Values of E_{vu} measured at several stress states during liquefaction process by large amplitude undrained cyclic shearing in tests 6 and 7 are plotted versus σ_v' and compared with those measured during isotropic consolidation in Fig. 11. It is seen that the E_{vu} values measured during liquefaction process were smaller than those during isotropic consolidation measured at the same σ_v'. It should be noted, however, that the σ_h' values during liquefaction process in test 6 were not always equal to σ_v', while those in test 7 were kept equal to σ_v'. The former stress states are different from those during isotropic consolidation, and this may result in a different ratio of E_{vu} to E_v. In the theory assuming a cross-anisotropic elastic body, the ratio changes depending on the values of $R=\sigma_v'/\sigma_h'$, as seen from Eqs. (8) and (9) in Appendix.

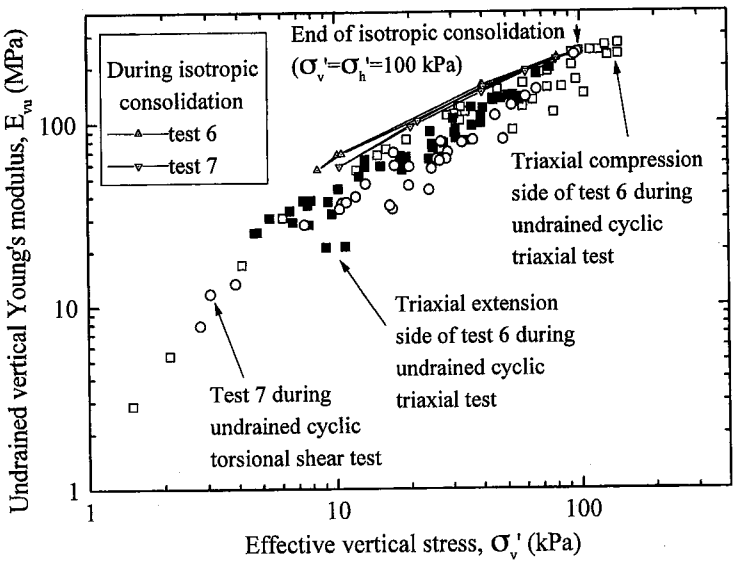

Figure 11. Undrained Young's modulus versus effective vertical stress

To correct for the above difference, by using Eqs. (8) and (9) under the condition as given in Appendix (i.e., a =1.1 and ν_0=0.15 with MP correction), values of E_v during liquefaction process in both tests were estimated from the above results and compared with those measured during isotropic consolidation in Fig. 12. It is seen that the estimated E_v values during liquefaction process were smaller than those during isotropic consolidation at the same σ_v'. It should be noted that the difference in the E_v values during these processes is over-estimated in the present study, because the E_v values were measured after aging for 30 minutes during isotropic consolidation, while no aging effects were involved during the liquefaction process.

When Figs. 11 and 12 are compared in detail, it is seen that the deviation in the values of Young's modulus under triaxial extension condition (i.e., R<1) in test 6 could be reduced by converting E_{vu} to E_v considering the effects of inherent and stress system-induced anisotropy and those of MP. On the other hand, possible reduction in the deviation under triaxial compression condition (R>1) was not clearly observed. It is also seen that the estimated E_v values under triaxial compression condition were generally larger than those under triaxial compression

condition. This may suggest that the extent of damage to the soil structure during liquefaction process by applying cyclic vertical loads is smaller under triaxial compression condition than under triaxial extension condition. The same trend of behavior has been observed on solid cylindrical specimens as reported by Koseki et al. (1998). It should also be noted that in test 7, the reduction in the E_v values during liquefaction process by applying cyclic torsional loads was comparable to that under triaxial extension condition in test 6.

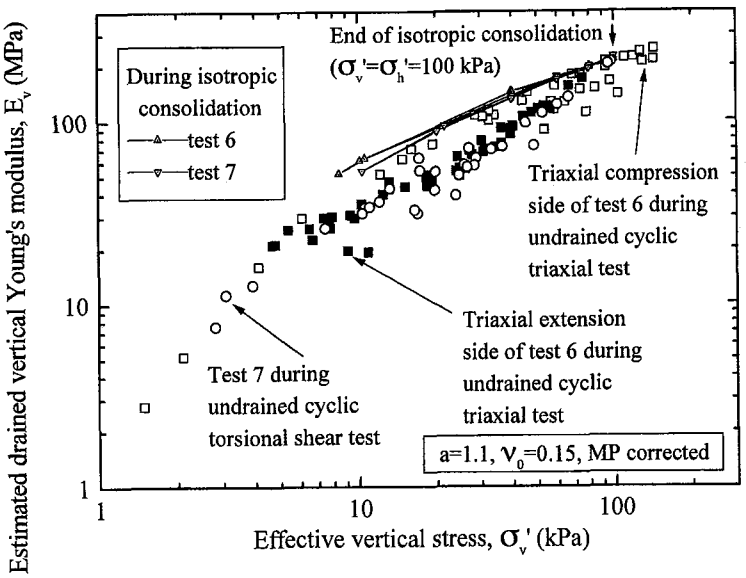

Figure 12. Estimated drained Young's modulus versus effective vertical stress

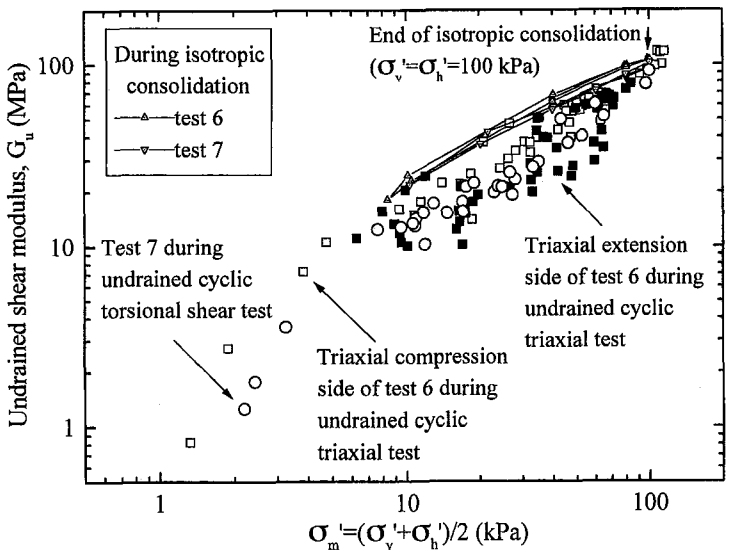

Figure 13. Undrained shear modulus versus effective mean stress, $\sigma_m'=(\sigma_v'+\sigma_h')/2$

Values of G_u measured at several stress states during liquefaction process by large amplitude undrained cyclic shearing in tests 6 and 7 are plotted versus $\sigma_m'=(\sigma_v'+\sigma_h')/2$ and compared with those measured during isotropic consolidation in Fig. 13. It is seen that, when compared at the same σ_m', the G_u values during liquefaction process in both tests became smaller than those during isotropic consolidation. The degree of degradation in the G_u values was almost the same as that in the E_v values as seen from Fig. 12, and effects of the different stress states (i.e., triaxial compression and extension conditions in test 6 and condition of $\sigma_v'=\sigma_h'$ in test 7) on the G_u values were also qualitatively similar to those previously mentioned on the E_v values. These behaviors may suggest that the damage to the soil structure during liquefaction process occurs in a similar manner with respect to the Young's modulus in the vertical direction and the shear modulus defined on vertical and horizontal planes that are orthogonal.

In Fig. 14, values of dp'/dq measured during undrained small cyclic vertical loading in test 6, which denotes the average direction of the effective stress path as typically shown in Fig. 7b, are plotted versus the current stress ratio R ($=\sigma_v'/\sigma_h'$) and compared to theoretical values calculated by using Eqs. (9) and (10) in Appendix. It is seen that, under the condition as employed in the previous calculation (i.e., a =1.1 and ν_0=0.15 with MP correction), the measured relationship could be reasonably simulated by the theory under triaxial compression condition, while under triaxial extension condition the measured value deviated largely from the theoretical one. The latter deviation may be related with the observation that the degradation in the values of E_v and G_u during liquefaction process was larger under triaxial extension condition than under triaxial compression condition (Figs. 12 and 13). Similar trend of behavior has been reported on solid cylindrical specimens by Koseki et al. (1998).

It should be noted that values of $dp'/d\tau$ measured during undrained small cyclic torsional loading as typically shown in Fig. 6b were always nearly zero. This behavior suggests that dilatancy was not mobilized during small cyclic torsional loading, resulting in almost the same values of G and G_u measured during isotropic consolidation (Fig. 10).

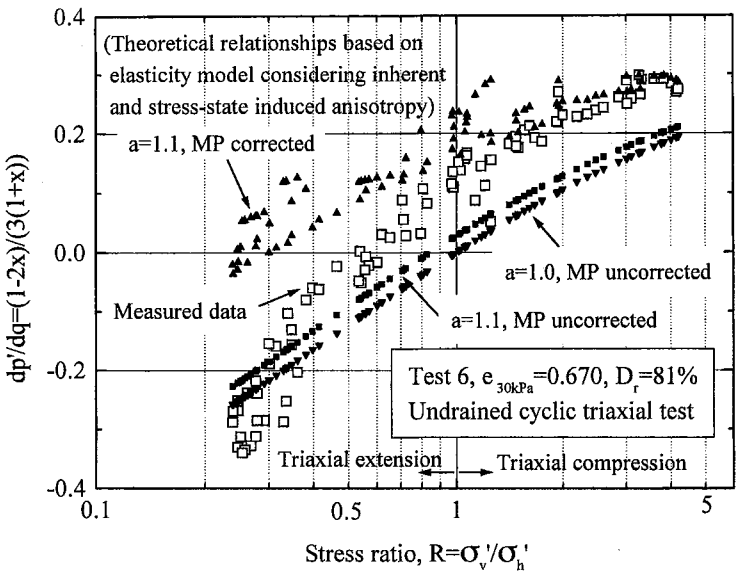

Figure 14. Direction of effective stress path during undrained small cyclic vertical loading

CONCLUSIONS

The results from large amplitude undrained cyclic torsional and triaxial tests on Toyoura sand measuring change of quasi-elastic deformation properties could be summarized as follows.

During isotropic consolidation, the drained and undrained shear moduli were almost the same irrespective of the drainage condition. The difference in the drained and undrained vertical Young's moduli that was measured during isotropic consolidation could be explained by considering inherent and stress state-induced anisotropy in modeling of elastic deformation characteristics and by correcting for the effects of membrane penetration.

During liquefaction process induced by undrained cyclic shearing, degradation in the elastic deformation properties was observed when compared to those measured during isotropic consolidation. The degree of degradation in the values of the shear modulus and the vertical Young's modulus was almost the same. Degradation during undrained cyclic torsional shear test was comparable to that under triaxial extension condition during undrained cyclic triaxial shear test, which was larger than that under triaxial compression condition during the latter test. Different extent of damage to soil structure during liquefaction process that depends on the stress state was suggested.

REFERENCES

Goto, S. (1986): "Strength and characteristics of granular materials in triaxial tests," Dr. of Eng. Thesis, University of Tokyo.

Hardin,B.O. and Richart,F.E. (1963): "Elastic wave velocities in granular soils," *J. Soil Mech. Found. Div.*, ASCE, Vol.89, No.SM1, pp.33-65.

Hoque E. and Tatsuoka, F. (1998): Anisotropy in elastic deformation of granular materials, *Soils and Foundations*, Vol. 38, No. 1, pp.163-179.

Koseki, J., Hamaya, S., Tatsuoka, F. and Maeshiro, N. (1998): "Elastoplastic deformation characteristics of Toyoura sand during liquefaction," *Geotechnical Engineering and Soil Dynamics III*, Geotechnical Special Publication No. 75, ASCE, Vol. 1, pp. 385-397.

Santucci de Magistris, F., Koseki, J., Amaya, M., Hamaya, S., Sato, T. and Tatsuoka, F. (1999): "A triaxial testing system to evaluate stress-strain behaviour of soils for wide range of strain and strain rate," *Geotechnical Testing Journal*, Vol. 22, pp. 44-60.

Tatsuoka, F. and Kohata, Y. (1995): "Stiffness of hard soils and soft rocks in engineering applications," *Pre-failure Deformation of Geomaterials*, Balkema, Vol. 2, pp. 947-1043.

Tatsuoka, F., Jardine, R.J., Lo Presti, D., Di Benedetto, H. and Kodaka, T. (1997): "Characterising the pre-failure deformation properties of geomaterials," *Theme lecture of 14th ICSMFE* (in print).

APPENDIX: MODELING OF ELASTIC DEFORMATION PROPERTIES

The cross-anisotropic elastic formulation employed to analyze the present results are briefly explained below, which is slightly modified from the one employed by Koseki et al. (1998) in terms of the effects of the membrane penetration to accommodate them to hollow cylindrical specimens.

It has been experimentally reported by Hoque and Tatsuoka (1998) that the elastic Young's modulus of granular materials is basically a function of the effective normal stress in the direction of the major

principal strain increment. Therefore, the drained vertical and horizontal Young's moduli, denoted as E_v and E_h, respectively, were formulated by Eqs. (1) and (2), as proposed by Tatsuoka and Kohata (1995):

$$E_v = E_{v0}(\sigma_v' / \sigma_0')^m \cdot f(e)/f(e_0) \quad \cdots(1)$$

$$E_h = E_{h0}(\sigma_h' / \sigma_0')^m \cdot f(e)/f(e_0) \quad \cdots(2)$$

where σ_0' and e_0 are the reference stress and void ratio, and $f(e)=(2.17-e)^2/(1+e)$ is the void ratio function to account for effects of void ratio changes (Hardin and Richart, 1963). These properties result in stress state-induced anisotropy in the elastic deformation characteristics (Tatsuoka and Kohata 1995).

By assuming a symmetricity for the elastic compliance matrix, the drained Poisson's ratios are assumed to be basically dependent on the current stress ratio $R=\sigma_v'/\sigma_h'$ as formulated by:

$$\nu_{vh} = \nu_0 \sqrt{a} \cdot R^{m/2}, \qquad \nu_{hv} = \nu_0 (1/\sqrt{a}) \cdot R^{-m/2} \quad \cdots(3), (4)$$

where a is a parameter representing the degree of inherent anisotropy ($a \equiv E_{v0}/E_{h0}$), and ν_0 is the value of $\nu_{vh}=\nu_{hv}$ when $R=a^{-1/m}$. In the present study, reference values of a and ν_0 were set to 1.1 and 0.15, respectively, based on the results by Hoque and Tatsuoka (1998). Further, the Poisson's ratio defined on two orthogonal horizontal planes ν_{hh} was assumed constant and equal to ν_0.

By using Eqs. (1) to (4), the elastic normal strain increments $d\varepsilon_v^e$ and $d\varepsilon_h^e$ in the vertical and horizontal directions, caused by effective stress increments $d\sigma_v'$ and $d\sigma_h'$, can be evaluated as:

$$d\varepsilon_v^e = \frac{1}{E_v} d\sigma_v' + 2\frac{\nu_{hv}}{E_h} d\sigma_h' \quad \cdots(5)$$

$$d\varepsilon_h^e = \frac{1+\nu_0}{E_h} d\sigma_h' + \frac{\nu_{vh}}{E_v} d\sigma_v' \quad \cdots(6)$$

In some cases, effects of membrane penetration were considered by formulating the apparent volumetric strain increment $d\varepsilon_{MP}$ due to membrane penetration by:

$$d\varepsilon_{MP} = \frac{4b}{\sigma_h' \cdot (d_o - d_i)} d\sigma_h' \quad \cdots(7)$$

where d_o and d_i are the outer and the inner diameters of the specimen in cm, and b is a parameter that was experimentally obtained by Goto (1986) to be $1.7\times10^3/\log_e 10$ for Toyoura sand.

Based on these assumptions, the theoretical relationship between the undrained and drained vertical Young's moduli, denoted as E_{vu} and E_v, respectively, at the same stress state was obtained by Tatsuoka et al. (1997) as:

$$E_v = E_{vu} \frac{1+2(aR^m)^{0.5}\nu_0 x}{1+x} \quad \cdots(8)$$

where x is the stress increment ratio during small cyclic vertical loading under undrained condition given by:

$$x = -\left(\frac{d\sigma_h'}{d\sigma_v'}\right) = \frac{1-2(aR^m)^{0.5}\nu_0}{2aR^m\left[1-\nu_0-(aR^m)^{-0.5}\nu_0+2(bE_h)/(\sigma_h'(d_o-d_i))\right]} \quad \cdots(9)$$

The ratio dp'/dq, which denotes the average direction of the effective stress path measured during undrained small cyclic vertical loading, as typically shown in Fig. 7b, can also be predicted as a unique function of x by:

$$\frac{dp'}{dq} = \frac{1-2x}{3(1+x)} \quad \cdots(10)$$